HHS Public Access

Author manuscript

Oncogene. Author manuscript; available in PMC 2016 July 08.

Published in final edited form as:

Oncogene. 2016 May ; 35(21): 2801–2812. doi:10.1038/onc.2015.330.

Ceramide limits phosphatidylinositol-3-kinase C2β-controlled cell motility in ovarian cancer: potential of ceramide as a metastasis-suppressor lipid

Kazuyuki Kitatani[1,2,*], **Usui Toshinori**[1], **Shravan Kumar Sriraman**[3], **Masafumi Toyoshima**[2], **Masumi Ishibashi**[2], **Shogo Shigeta**[2], **Satoru Nagase**[4], **Masahiro Sakamoto**[2], **Hideo Ogiso**[5], **Toshiro Okazaki**[5,6], **Yusuf A. Hannun**[7], **Vladimir P. Torchilin**[3], and **Nobuo Yaegashi**[1,2]

[1]Tohoku Medical Megabank Organization, Tohoku University Graduate School of Medicine, Tohoku University, Sendai, Japan

[2]Department of Obstetrics and Gynecology, Tohoku University Graduate School of Medicine, Tohoku University, Sendai, Japan

[3]Department of Pharmaceutical Sciences, Center for Pharmaceutical Biotechnology and Nanomedicine, Northeastern University, Boston, MA, USA

[4]Department of Obstetrics and Gynecology, Yamagata University, Stony Brook, NY, USA

[5]Department of Life Science, Medical Research Institute, Kanazawa Medical University, Stony Brook, NY, USA

[6]Department of Medicine, Division of Hematology/Immunology, Kanazawa Medical University, Stony Brook, NY, USA

[7]Stony Brook Cancer Center and Department of Medicine, Stony Brook University, Stony Brook, NY, USA

Abstract

Targeting cell motility, which is required for dissemination and metastasis, has therapeutic potential for ovarian cancer metastasis, and regulatory mechanisms of cell motility need to be uncovered for developing novel therapeutics. Invasive ovarian cancer cells spontaneously formed protrusions, such as lamellipodia, which are required for generating locomotive force in cell motility. siRNA screening identified class II phosphatidylinositol 3-kinase C2β (PI3KC2β) as the predominant isoform of PI3K involved in lamellipodia formation of ovarian cancer cells. The bioactive sphingolipid ceramide has emerged as an antitumorigenic lipid, and treatment with short-chain C_6-ceramide decreased the number of ovarian cancer cells with PI3KC2β-driven lamellipodia. Pharmacological analysis demonstrated that long-chain ceramide regenerated from C_6-ceramide through the salvage/recycling pathway, at least in part, mediated the action of C_6-

*Corresponding Author: Kazuyuki Kitatani, Ph.D., Tohoku Medical Megabank Organization, Department of Obstetrics and Gynecology, Tohoku University Graduate School of Medicine, Tohoku University, 2-1 Seiryomachi, Aoba-ku, Sendai 980-0873, Japan. Tel: +81-022-717-7251; FAX: +81-022-717-7258; kitatani@med.tohoku.ac.jp.

Disclosure of Potential Conflict of Interest: The authors declare no conflicts of interest.

ceramide. Mechanistically, ceramide was revealed to interact with the PIK-catalytic domain of PI3KC2β and affect its compartmentalization, thereby suppressing PI3KC2β activation and its driven cell motility. Ceramide treatment also suppressed cell motility promoted by epithelial growth factor, which is a prometastatic factor. To examine the role of ceramide in ovarian cancer metastasis, ceramide liposomes were employed and confirmed to suppress cell motility *in vitro*. Ceramide liposomes had an inhibitory effect on peritoneal metastasis in a murine xenograft model of human ovarian cancer. Metastasis of PI3KC2β knocked-down cells was insensitive to treatment with ceramide liposomes, suggesting specific involvement of ceramide interaction with PI3KC2β in metastasis suppression. Our study identified ceramide as a bioactive lipid that limits PI3KC2β-governed cell motility, and ceramide is proposed to serve as a metastasis-suppressor lipid in ovarian cancer. These findings could be translated into developing ceramide-based therapy for metastatic diseases.

Keywords

cell motility; ceramide; ovarian cancer; phosphoinositide 3-kinase C2β; metastasis and dissemination

Introduction

Ovarian cancer is a frequent cancer among women and causes more deaths per year than any other female reproductive cancer. It usually disseminates and metastasizes widely, significantly increasing mortality and decreasing quality of life.[1-4] To overcome those clinical difficulties, it is important to develop novel pharmacotherapeutics to counter dissemination and metastasis of ovarian cancer.

Establishment of cancer dissemination and metastasis requires cell motility.[5, 6] Cancer cells migrate when their actin cytoskeleton is reorganized for promotion of cell motility. Localized actin polymerization at the leading edge pushes the membrane forward in finger-like structures known as filopodia and sheet-like structures known as lamellipodia.[7, 8] These pseudopodia generate the locomotive force in the migrating cells. Increased membrane pseudopodia elicited by growth factor stimulation in two-dimensional cell culture have been shown to represent closely enhanced three-dimensional migration properties of invasive cells.[9] Thus, cancer cell motility governed by pseudopodia formation is a strong candidate as a therapeutic target for cancer metastasis.

Sphingolipids are based on long-chain sphingoid bases (sphingosine or dihydrosphingosine), and ceramide, a central lipid in the metabolism of sphingolipids, has emerged as an important bioactive lipid that modulates cell death, cell cycle arrest, stress responses, and proinflammatory responses.[10-14] Several enzymes are involved in forming ceramide[15], and ceramide synthase[11, 16] is a key enzyme in the *de novo* pathway or the salvage/recycling pathway of ceramide synthesis.[11] A growing body of evidence has demonstrated roles of ceramide salvage/recycling pathway in many biological responses, such as proinflammatory responses[17], growth arrest,[18] apoptosis,[19] cellular signaling,[20] and trafficking.[21] Therefore, the pathobiological role of ceramide has been extensively studied.

Ceramide has been characterized as an apoptosis-inducing molecule in cancer cell biology.[22] Preclinical studies using ceramide-formulated nanoscale liposomes have demonstrated that ceramide serves as an antitumorigenic lipid *in vivo*, and have suggested that ceramide-based therapy is effective against tumor growth.[23-28]

It remains to be determined whether ceramide is involved in regulatory mechanisms of cancer metastasis. Recently, downregulation of ceramide synthase 6 was reported to increase cell motility during epithelial–mesenchymal transition (EMT)[62], although its molecular mechanism and significance in metastasis remain to be clarified. Therefore, further understanding the significance of ceramide in cancer cell motility and metastasis could raise the potential of ceramide-based therapies for metastatic diseases.

Accumulating evidence is emerging that the phosphatidylinositol 3-kinase (PI3K)–Akt pathway plays important roles in cancer cell growth and motility,[29] and this pathway is frequently active in ovarian cancer and is proposed to be a therapeutic target.[30, 31] Extensive research has identified ceramide-interacting proteins that account for ceramide-transmitted biological responses. Ceramide has been shown to facilitate dephosphorylation and inactivation of oncogenic Akt by activating ceramide-activated protein phosphatases such PP2A.[32, 33] Therefore, ceramide might limit PI3K–Akt-driven cell motility in ovarian cancer progression and metastasis.

In this study, for the first time, we uncovered the regulatory mechanism by which ceramide limits cell motility and propose that ceramide serves as a metastasis-suppressor lipid in ovarian cancer.

Results

Identification of PI3K catalytic subunits responsible for forming lamellipodia

The formation of pseudopodia plays a role in cell migration and motility,[34] which is a critical step in the dissemination and metastasis of cancer cells. Invasive SKOV3 ovarian cancer cells form pseudopodia,[35] and the PI3K–Akt pathway has been implicated in forming lamellipodia.[36] Cells were stained with phalloidin for visualizing F-actin, which identified F-actin-enriched pseudopodia such as lamellipodia and filopodia. 26.6% of SKOV3 cells formed lamellipodia in medium supplemented with 10% serum, and the number of cells forming lamellipodia decreased by 3.7% with serum starvation (Supplementary Figure 1), showing that SKOV3 cells form lamellipodia in a serum-dependent manner. Furthermore, inhibition of PI3K by wortmannin abolished Akt phosphorylation at residue Ser^{473} and decreased formation of lamellipodia (Figure 1A and B), suggesting PI3K-dependent formation of lamellipodia in the presence of serum.

PI3K consists of catalytic and regulatory subunits, and eight isoforms of the former subunits have been identified.[37] To determine which catalytic isoform is predominantly responsible for the formation of lamellipodia, effects of individual siRNAs on the formation of lamellipodia were assessed. The knockdown of *PIK3C2B* (PI3KC2B) or *PIK3C1D* (PI3K p110δ) genes significantly inhibited the formation of lamellipodia, and the former siRNA treatment was most effective (Figure 1C and D). The effectiveness of their siRNAs was

confirmed (Figure 1E). Collectively, these results suggest that PI3KC2β, a gene product of *PIK3C2B*, is predominantly responsible for the formation of lamellipodia representing cell motility.

Short-chain ceramide treatment diminishes ovarian cancer cell motility

Ceramide has been implicated in the regulatory mechanisms of the PI3K–Akt signaling pathway. Treatment of SKOV3 cells with a short chain C_6-ceramide for 3 h decreased the number of cells forming lamellipodia identified by phase-contrast microscopy (Supplementary Figure 2). We further evaluated the effects of ceramide on other cancer cell lines such as TOV112D ovarian cancer cells and highly metastatic MDA-MB-231 breast cancer cells. SKOV3 and MDA-MB-231 cells both predominantly formed lamellipodia, and TOV112D cells formed filopodia. C_6-ceramide treatment suppressed the formation of pseudopodia in all cell lines (Figure 2A). The inhibitory effects of C_6-ceramide on formation of pseudopodia, such as lamellipodia and filopodia, were suspected to result in decreased cell motility and migration. We determined the cellular pharmacodynamics of C_6-ceramide toward pseudopodia formation. The number of SKOV3 cells forming lamellipodia significantly began to decline after 3 h treatment with C_6-ceramide (Figure 2B). In addition, C_6-ceramide treatment decreased the number of cells forming lamellipodia in a dose-dependent manner, with an IC_{50} value of ~2 μM (Figure 2C).

We further tested the effects of ceramide on cell motility in a Transwell migration assay. Treatment of invasive ovarian cancer SKOV3 cells with C_6-ceramide inhibited cell migration in a dose-dependent manner (Supplementary Figure 3). The data were further fitted using GraphPad Prism to determine the IC_{50}, which showed a value of 3.8 μM.

Ceramide is known as an apoptosis-inducing lipid. However, 9 h treatment with up to 30 μM C_6-ceramide, which was an experimental condition used for a cell motility assay, did not cause cell death (Supplementary Figure 4A) and PARP cleavage, which is a biochemical characteristic of apoptosis (Supplementary Figure 4B). C_6-ceramide also had no effects on cellular levels of ATP, which is a prerequisite for F-actin formation (Supplementary Figure 5). These findings suggest that ceramide selectively has an inhibitory effect on the signaling responsible for promoting cell motility.

To examine inhibitory effects of ceramide on cell motility in noncancerous cells, immortalized ovarian surface ovarian epithelial cells (OSE4)[38] were used. C_6-ceramide treatment suppressed the motility, and its IC50 value was 14.6 μM (Supplementary Figure 6). Noncancerous immortalized cells appear to be less sensitive to C6-ceramide as compared with SKOV3 ovarian cancer cells (Figure 2C).

Constitutive turnover of sphingolipids occurs in living cells, and a short-chain C_6-ceramide is converted to sphingosine, long-chain ceramide and its metabolites through the recycling pathway.[11] To identify sphingolipids responsible for inhibiting cell motility in C_6-ceramide-treated cells, mass spectrometric analysis of C_6-ceramide metabolism and pharmacological approaches were used. C_6-ceramide treatment increased ceramides, hexosylceramides, and sphingosine, but not sphingomyelin (Figure 3A–D). Inhibition of C_6-ceramide recycling by ceramide synthase inhibitor fumonisin B1[11, 39] in C_6-ceramide-treated cells suppressed the

formation of ceramide and hexosylceramide, and conversely potentiated the formation of sphingosine. These results suggest that C_6-ceramide is, at least in part, converted to long-chain ceramide and hexosylceramide through the recycling pathway.

Importantly, inhibition of C_6-ceramide recycling by fumonisin B1, partially and significantly, restored the formation of lamellipodia from 12.8% to 23.8% in C_6-ceramide-treated cells (Figure 3E and F). Consistently, cell migration in C_6-ceramide-treated cells was also recovered by fumonisin B1 (Figure 3G). Glucosylceramide synthase converts ceramide to glucosylceramide that serves as a precursor for complex glycosphingolipids. Inhibition of glucosylceramide synthase by N-butyldeoxynojirimycin is assumed to increase ceramide and decrease glucosylceramide and complex glycosphingolipids. Substantially, its treatment *per se* reduced the number of cells forming lamellipodia, probably because of increased ceramide. N-butyldeoxynojirimycin had no significant effects on cell motility in C_6-ceramide-treated cells (Figure 3H and I), ruling out involvement of glucosylceramide and complex glycosphingolipids in anti-motility activities of C_6-ceramide.

C_6-ceramide can also be converted to C_6-sphingomyelin, but this reaction is not inhibited by fumonisin B1. Treatment with exogenous 10 μM C_6-sphingomyelin had no significant effects on cell migration (Figure 3J) and lamellipodia formation (data not shown), ruling out involvement of sphingomyelin in C_6-ceramide-dependent inhibition of cell motility. In addition, C_6-ceramide is not a substrate preferred for ceramide kinase,[40] implying less involvement of ceramide-1-phosphate.

Collectively, C_6-ceramide and long-chain ceramide generated through the recycling pathway are suggested to function primarily as inhibitory lipids in cell motility.

Ceramide inhibits the PI3K pathway responsible for cell motility

Ceramide has a potent inhibitory effect on PI3K-controlled cell motility. C_6-ceramide treatment reduced cellular amounts of phosphatidylinositol 3-phosphate, which is a metabolic product of PI3KC2β (Figure 4A). PI3KC2β products such as phosphatidylinositol 3-phosphate are known to bind and activate PH domain-containing Akt. Consistent with phosphatidylinositol 3-phosphate reduction, C_6-ceramide treatment decreased phosphorylated/active Akt at residues Thr^{308} and Ser^{473} in a dose-dependent manner (Figure 4B). Fumonisin B1 treatment restored phosphorylation of Akt at residue Ser^{473} in C_6-ceramide-treated cells (Figure 4C), also implying an involvement of recycled ceramide in the regulatory mechanism of the PI3K–Akt pathway. These results suggest that ceramide selectively suppresses the PI3K–Akt pathway responsible for cell motility of ovarian cancer cells.

Overexpression of epidermal growth factor (EGF) receptor by ovarian tumors is associated with more aggressive clinical behavior and correlates with poor prognosis.[41, 42] The EGF–EGF receptor axis is implicated in dissemination and metastasis of ovarian cancer.[43] This EGF signal activates the PI3K–Akt pathway, thereby promoting lamellipodia formation and cell motility.[36, 44] Treatment of SKOV3 cells with EGF for 5 min showed a 45% increase in lamellipodia formation, and 10 μM C_6-ceramide treatment potently blocked the formation of lamellipodia in EGF-stimulated cells (Figures 4D and 3E). Immunofluorescence microscopy

showed Akt relocalization to tubular-shaped compartments enriched with F-actin in EGF-treated cells, and C_6-ceramide blocked its relocalization (Supplementary Figure 7). EGF treatment increased phosphorylation of Akt, ERK1/2, and EGF receptor, and C_6-ceramide treatment selectively and significantly suppressed EGF activation of Akt at residues Thr^{308} and Ser^{473} (Figure 4F), which was consistent with lamellipodia formation (Figure 4D and E). These results suggest that ceramide specifically targets the PI3K responsible for cell motility and acts in the signal pathway transducing receptors such as EGF receptor to PI3K.

Ceramide promotes the activity of serine/threonine protein phosphatase PP2A that is responsible for dephosphorylation of Akt.[22, 45] The effect of ceramide on Akt dephosphorylation is specific to Ser^{473} but not Thr^{308}. To clarify the involvement of ceramide-activated protein phosphatases[46, 47] in decreasing phosphorylation of Akt at Thr^{473}, the effects of specific inhibitors for PP2A on Akt dephosphorylation were tested. Inhibition of PP2A by 10 nM okadaic acid (IC50 for PP2A = 1.2 nM)[48] or 1 nM calyculin A (IC50 for PP2A = 0.5-1.0 nM)[49] failed to restore Akt phosphorylation in C_6-ceramide-treated cells (Supplementary Figure 8). These results argue against but do not totally rule out involvement of ceramide-activated PP2A in mediating ceramide-dependent decrease in Akt phosphorylation.

PTEN is a well-established tumor suppressor gene, and its biochemical function preferentially counteracts the activity of the class I PI3K by degrading its metabolite phosphatidylinositol-3,4,5-trisphosphate to form phosphatidylinositol-4,5-bisphosphate.[50] PTEN is thought to be involved in Akt inactivation by ceramide, but PTEN-silenced cells still displayed ceramide-dependent inactivation of Akt (Supplementary Figure 9). These results rule out involvement of PTEN in ceramide inactivation of Akt.

Ceramide targets PI3KC2β and limits cell motility

The results above demonstrate that ceramide limits cell motility predominantly governed by PI3KC2β. To uncover whether ceramide is involved in the regulatory mechanism of PI3KC2β-driven cell motility, V5-tagged PI3KC2β expression vector was constructed to determine the effects of ceramide on PI3KC2β-promoted cell motility (Figure 5A). In vehicle (0.1% ethanol)-treated cells, enforced expression of PI3KC2β significantly increased the formation of lamellipodia by 26.3% as compared with empty vector expression, and importantly C_6-ceramide treatment prevented the significant increases in lamellipodia formation by PI3KC2β overexpression (Figure 5B). These results suggest that ceramide specifically suppresses PI3KC2β-driven formation of lamellipodia. Indirect immunofluorescence confocal microscopy showed that phosphorylated Akt (Ser^{473}) at the lamellipodia was increased in PI3KC2β-transfected cells compared with empty-vector-transfected cells (Figure 5C). Moreover, C_6-ceramide treatment reduced the phosphorylation of Akt.

Ceramide either directly or indirectly interacts with C2-domain-containing proteins such as PKCα[51, 52] and cytosolic phospholipase A_2 [53], and PI3KC2β contains this domain. These considerations raised the potential of PI3KC2β as a ceramide-interacting protein. To test this, we used a pull-down assay using biotin-conjugated C_6-ceramide. Biotin-conjugated C_6-

ceramide specifically interacted with PI3KC2β and PKCα, but not other proteins such as PI3K p110α and β-actin (Figure 5D).

P13KC2β[37, 54, 55] consists of three domain including two C2 domains and a PIK-catalytic domain. Three types of domain deletion mutants (termed C2B deletion, PIK-catalytic, and C2A) were constructed to identify the binding domain of ceramide in PI3KC2β (Figure 5D). Biotin-conjugated C_6-ceramide was revealed to interact specifically with full-length PI3KC2β and two types of mutants including C2B deletion and PIK-catalytic domain, but not C2A mutant (Figure 5E), thereby suggesting that PIK-catalytic domain is responsible for interacting with ceramide.

To uncover the significance of this interaction in catalytic activity, the effects of ceramide on *in vitro* PI3KC2β activity were tested. Ceramide had no inhibitory effects on kinase activities of PI3KC2β and other PI3Ks (Supplementary Table 1).

It is possible that ceramide affects compartmentalization of PI3KC2β. Full-length PI3KC2β in vehicle (ethanol)-treated cells was localized in lamellipodia characterized with F-actin enrichment. Treatment with C_6-ceramide led to relocalization of full-length PI3KC2β away from lamellipodia, coincident with disappearance of the lamellipodia (Figure 5F). Similar to full-length PI3KC2β, two ceramide-interacting mutants, including C2B deletion and PIK-catalytic, were also lamellipodium-resident and sensitive to C_6-ceramide treatment. Therefore, ceramide interaction with PIK-catalytic is suggested to account for PI3KC2β relocalization away from lamellipodia.

Ceramide is suggested to interact with PI3KC2β *via* the PIK-catalytic domain and in turn suppress cell motility by causing its relocalization away from lamellipodia.

p110δ is also responsible for cell motility (Figure 1). To clarify whether ceramide targets p110δ in the regulatory mechanism of cell motility, we investigated the interaction of p110δ with ceramide. Similar to PI3KC2β, V5-tagged p110δ interacted with biotinylated C_6-ceramide (Supplementary Figure 10A). Moreover, V5-tagged p110δ was localized in lamellipodia and treatment with C_6-ceramide led to its relocalization away from lamellipodia (Supplementary Figure 10B). These results suggest that ceramide–p110δ interaction also has an inhibitory effect on cell motility.

Potential of ceramide as a metastasis suppressor in ovarian cancer

To investigate the role of ceramide in ovarian cancer metastasis, ceramide liposomes are used. Liposomes as nanocarriers are used for drug delivery[56], and functional liposomes such as ceramide liposomes have therapeutic effects in cells or animal models.[24, 26, 57] Our group recently established transferrin- and octadecylrhodamine-B-conjugated C_6-ceramide liposomes (C_6-Cer TLs) for targeting cancer cells abundantly expressing transferrin receptors, and demonstrated that the liposomes initiated apoptosis of ovarian cancer cells *in vitro* and *in vivo*.[27] Therefore, ceramide liposomes are exploited to not only evaluate ceramide-based therapy, but also define a role for ceramide in cancer *in vivo*.

To confirm antimetastatic activities of C_6-Cer TLs in a cell model, SKOV3 cells were treated with ceramide-free liposomes (TLs) or C_6-Cer TLs for 12 h. Confocal microscopy showed

that TLs and C_6-Cer TLs were both incorporated into SKOV3 cells (Figure 6A). Importantly, the formation of lamellipodia was suppressed in cells treated with C_6-Cer TLs (Figure 6A). The number of cells forming lamellipodia in liposome-treated cells was determined. As shown in Figure 6B, 10 μM C_6-ceramide-containing C_6-Cer TLs significantly reduced the formation of lamellipodia by 60% relative to that of TLs. Consistent with cell motility, treatment with C_6-Cer TLs decreased phosphorylation of Akt at Ser^{473} in a dose-dependent manner (Figure 6C and D). Those results demonstrate that ceramide liposomes have an inhibitory effect on PI3K-driven cell motility.

To test the effects of ceramide liposomes on ovarian cancer metastasis *in vivo*, a human ovarian cancer xenograft model was used. Inoculation of SKOV3 cells into the peritoneal cavity of nude mice led to the generation of metastatic nodules in the mesentery, and liposome treatment had no effect on body weight (Figure 6E and F). The number of metastatic nodules in TL-treated mice was 64.3 ± 7.2/mouse, and importantly, C_6-Cer TL treatment significantly inhibited the formation of metastatic nodules by 33.3% or 26.1% as compared with TLs or PBS (control), respectively (Figure 6F and G). These results demonstrated that C_6-Cer TLs had an inhibitory effect on peritoneal dissemination and metastasis in an ovarian cancer xenograft model. These results suggest that ceramide serves as a metastasis-suppressor lipid in ovarian cancer.

In a cell model, ceramide specifically limits PI3KC2β-governed cell motility. To confirm the *in vivo* significance of ceramide–PI3KC2β interaction in suppressing metastasis of ovarian cancer, we examined the effects of C_6-Cer TLs on metastasis in PI3KC2β-silenced cells *in vivo*. At first, *in vitro* effects of ceramide on cell motility were determined in PI3KC2β-silenced cells. In the migration assay, PI3KC2β-knocked-down cells were less sensitive to C_6-ceramide compared with control-2 siRNA-treated cells. However they were still substantially sensitive to C_6-ceramide to some extent (Figure 7A). This remaining sensitivity to C_6-ceramide might be attributed to ceramide–p110β interaction.

To determine *in vivo* effects of C_6-Cer TLs on metastasis of PI3KC2β-silenced cells, we used siRNA for PI3KC2β knockdown. SKOV3 cells were transfected with control-2 or PI3KC2β siRNAs for 24 h and then transfection reagents were removed. The significant effectiveness of PI3KC2β knockdown was confirmed to persist for up to 3 days (Figure 7B).

Transfected cells were inoculated into the peritoneum of nude mice. PI3KC2β knockdown *per se* resulted in significant suppression in the number of metastatic nodules, showing *in vivo* effectiveness of PI3KC2β siRNAs and involvement of PI3KC2β in metastasis of ovarian cancer (Figure 7C). The siRNA-transfected SKOV3-xenografted mice were treated with TLs or C_6-Cer TLs continuously for 3 days after inoculation. C_6-Cer TL treatment had no significant effects on metastasis in PI3KC2β-silenced cells. These results suggest that ceramide–PI3KC2β interaction plays roles in suppressing metastasis of ovarian cancer *in vivo*.

Discussion

In the present study, we identified ceramide as an inhibitory lipid in regulatory mechanisms of PI3K-controlled motility and ceramide is proposed to serve as a tumor-suppressor lipid in ovarian cancer. These findings suggest the potential of ceramide-based therapy for prevention and/or treatment of ovarian cancer metastasis.

The initial cellular events required for metastasis are triggered by a switch from an epithelial cell type to a less differentiated mesenchymal one, which is known as EMT.[58] Cells undergoing EMT reorganize their cytoskeletons and extend protrusions such as pseudopodia, allowing for increased migratory capacity.[58] Those events could lead to cancer invasion and metastasis. Therefore, uncovering the regulatory mechanisms of pseudopodia formation is of critical importance to understanding cancer metastasis and discovering novel therapeutics.

The PI3K pathway is aberrantly activated in ovarian cancer, thereby emerging as a therapeutic target.[2, 31] In particular, class I PI3K catalytic isoforms have been well studied. siRNA screening identified class II PI3KC2β as a predominant catalytic isoform responsible for serum-dependent formation of lamellipodia (Figure 1), suggesting PI3KC2β-dependent cell motility in ovarian cancer. Importantly, PI3KC2β silencing had an inhibitory effect on metastasis of ovarian cancer (Figure 7). This isoform and its product phosphatidylinositol 3-phosphate have been also implicated in cell migration induced by lysophosphatidic acid[59] that stimulates survival, proliferation, migration and invasion of ovarian cancer cells.[60] Boller *et al.* have demonstrated not only that PI3KC2β is overexpressed in tumor samples and cell lines of acute myeloid leukemia and brain, but also that PI3KC2β inhibition leads to apoptosis.[61] As specific involvement of PI3KC2β and p110δ in progression and metastasis of ovarian cancer remains to be fully established, intensive investigation is needed to determine the clinical significance of those ceramide-interacting proteins in ovarian cancer.

Cancer cells contain ceramide, which consists of a sphingoid base attached to long- or very-long-chain free fatty acids via an amide bond. The natural ceramide is hydrophobic, although short chain C_6-ceramide is cell permeable. C_6-ceramide incorporated into cells is metabolized to form long-chain ceramide such as C_{16}-ceramide through the salvage/recycling pathway in cancer cells.[11] The recycling pathway of C_6-ceramide contributes, at least in part, to the response to C_6-ceramide in the suppression of cell motility (Figure 3), thus, demonstrating that the observed effects are mediated by endogenous natural ceramides. Ceramide synthase, which is a target of fumonisin B1, catalyzes the formation of long-chain ceramide in the recycling pathway of C_6-ceramide. Recently, Edmond *et al.* demonstrated that the ceramide synthase 6/C_{16}-ceramide pathway reduces cell motility,[62] which is consistent with our characterization of ceramide as an inhibitory lipid in cell motility. These findings implicate a novel role for the salvage/recycling pathway for ceramide synthesis in the regulatory mechanisms of cancer cell motility.

Several ceramide target proteins have been identified, including PKCα, PKCζ, PP2A, I2PP2A, cRaf, and kinase suppressor of Ras.[11, 63] Ceramide affects catalytic activities and/or compartmentalization of its target proteins. Here, for the first time, we identified PI3KC2β and p110δ as novel ceramide-interacting proteins (Figure 5). This ceramide-

PI3KC2β interaction is suggested to affect compartmentalization and suppress subsequent activation of PI3KC2β, thereby inhibiting cell motility and metastasis. The biological significance of ceramide interaction with PI3KC2β was partially disclosed and describing the dynamic interaction remains a challenge to structural biology.

We demonstrated that ceramide liposomes exhibit a strong inhibitory effect on cell motility (Figure 6). Similar to A2780 ovarian cancer cells,[27] SKOV3 cells are assumed to take up C_6-Cer TLs via transferrin receptors, because those cell lines abundantly express transferrin receptor 1.[64] The transferrin–transferrin receptor complex is internalized via clathrin-coated pits and passes through early endosomes to recycling endosomes. However, a significant portion of transferrin liposomes is trapped in endolysosomal compartments owing to octadecyl-rhodamine B modification of the liposomes for lysosomal targeting.[27] Indeed, the endolysosomal targeting of C_6-Cer TLs was effective against PI3KC2β–controlled cell motility, similar to C_6-ceramide treatment. Although the metabolic mechanism remains not fully known, the catalytic action of acid ceramidase in endolysosomes is assumed to account for degrading some liposomal C_6-ceramides to form sphingosine that serves as substrate for ceramide synthase. Collectively, lysosomal C_6-ceramide is presumably converted to long-chain ceramide through the salvage/recycling pathway, probably yielding anti-cell motility activity of C_6-Cer TLs.

Our studies in a mouse model also provide evidence indicating the therapeutic efficacy of ceramide liposomes against metastasis of ovarian cancer and demonstrate the significance of ceramide-PI3KC2β interaction in the anti-metastatic activities (Figures 6 and 7). Previously, *in vivo* studies of ceramide liposomes used in the present study have shown therapeutic efficacy against tumor growth in an ovarian cancer xenograft mouse model.[27] Collectively, ceramide liposomes are believed to have multiple activities against the progression of ovarian cancer.

The clinical relevance of ceramide levels in tumor progression remains to be fully studied. In human head and neck squamous cell carcinoma, the levels of C_{18}-ceramide were decreased in the tumor tissues, and decreased levels of C_{18}-ceramide were significantly associated with higher incidence of pathological nodal metastasis.[65] These findings indicate the possible clinical significance of ceramide reduction in cancer metastasis, and encourage the development of ceramide-based therapy for dissemination and metastasis in ovarian cancer.

In summary, ceramide is proposed to function as a bioactive lipid that inhibits PI3KC2β-controlled motility of ovarian cancer cells and serve as a metastasis suppressor. Our studies indicate the need to develop ceramide-based therapy for ovarian cancer metastasis.

Materials and Methods

Antibodies and reagents

PKCα antibody (sc208) and horseradish-peroxidase-conjugated antibodies for mouse (sc2005) and rabbit IgG (sc2004) were from Santa Cruz Biotechnology (Dallas, TX, USA). Fumonisin B1 was purchased from Alexis (San Diego, CA, USA). Mouse monoclonal V5 antibodies (R960-25), RNAiMax, Alexa Fluor488-conjugated phalloidin,

Lipofectamine2000, and siRNAs for the catalytic subunits of PI3K family were from Life Technologies. Tetramethylrhodamine isothiocyanate (TRITC)-conjugated phalloidin, biotin and β-actin antibodies (A5441) were from Sigma (St Louis, MO, USA). Hoechst 33342 was from Dojindo (Kumamoto, Japan). C_6-ceramide and C_6-sphingomyelin were from Matreya (Pleasant, PA, USA). Recombinant human EGF was from Peprotech (Rocky Hill, NJ, USA). Antibodies specific for p110α (#4249), EGF receptor (#2232), phospho-EGF receptor at Tyr^{845} (#2231), phospho ERK1/2, ERK1/2, Akt (#9272), phospho-Akt at Thr^{308} (#2965) or Ser^{473} (#9271) were from Cell Signaling Technology (Boston, MA, USA). Streptavidin-conjugated magnetic beads, SuperSignal West Dura Extended Duration Substrate, and Halt Phosphatase Inhibitor Cocktail were from Thermo Fisher Scientific (Rockford, IL, USA). Antibodies for p110δ (ab32401) and PI3KC2β (ab140525) were from Abcam (Cambridge, MA, USA). Phosphatidylinositol 3-phosphate ELISA kit and biotin-conjugated C_6-ceramide were from Echelon (Salt Lake City, UT, USA). Human PI3KC2β cDNA was a gift from Dr. Alexandre Arcaro (Universität Bern, Switzerland).

Cell culture

Ovarian cancer cell lines SKOV3 and TOV112D were kindly provided by Dr. Carla Grandori (Fred Hutchinson Cancer Research Center, Seattle, WA, USA) and grown in Dulbecco's modified Eagle's medium (DMEM) supplemented with 10% fetal bovine serum (FBS). Those cell lines were authenticated by JCRB Cell Bank (Osaka, Japan). MDA-MB-231 breast cancer cells were from the American Type Culture Collection and grown in RPMI 1640 medium supplemented with 10% FBS. OSE4 cells cultured in DMEM supplemented with 10% FBS were gifted from the Department of Obstetrics and Gynecology, Kumamoto University, Japan. Cells were maintained at <80% confluence under standard incubator conditions (humidified atmosphere, 95% air, 5% CO_2, 37°C). No mycoplasma contamination was observed in all cell lines.

Immunoblotting

Cells were washed three times with PBS supplemented with Halt Phosphatase Inhibitor Cocktail and lysed using Laemmli buffer. The protein samples (20 μg) were subjected to SDS-PAGE (4–20% gradient gels). Proteins were electrophoretically transferred to nitrocellulose membranes, blocked with PBS/0.1% Tween 20 (PBS-T) containing 5% nonfat dried milk, washed with PBS-T, and incubated with antibodies for Akt1 (1 in 1000 dilution), phospho-Akt (1 in 1000 dilution), ERK1/2 (1 in 1000 dilution), phospho-ERK1/2 (1 in 1000 dilution), or EGF (1 in 1000 dilution) in PBS-T containing 5% nonfat dried milk. The phospho-EGF receptor antibody (1 in 1000 dilution) was diluted with PBS-T containing 2% bovine serum albumin. The blots were washed with PBS-T and incubated with a secondary antibody conjugated with horseradish peroxidase in PBS-T containing 5% nonfat dried milk. Detection was performed using enhanced chemiluminescence reagent, and quantification of the chemiluminescent signals was performed with a digital imaging system.

Analysis of pseudopodia formation

Cells growing on glass-bottom dishes were treated with sphingolipids. After incubation, cells were washed with PBS twice and fixed with 4% formaldehyde for 10 min. Fixed cells were further treated with 0.1% TritonX-100 for 10 min followed by staining with Hoechst

33342 and TRITC-conjugated phalloidin for 5 min. For analysis of pseudopodia, including filopodia and lamellipodia, samples were examined with confocal microscopy. Lamellipodia are thin and veil-like extensions at the edge of cells that contain a dynamic array of actin filaments, and are biologically characterized with enrichment of F-actin. Cells were counted as having formed lamellipodia if there was an increase in visualized F-actin in the lamellipodia. The formation of lamellipodia was assessed by blinded quantification of fluorescence microscopy (each sample of >300 cells). Two investigators independently assessed the formation of lamellipodia.

Cell migration assay

Cells were plated onto the Transwell chambers. The migratory cells attached to the lower surface were stained with Hoechst 33342, and the imaging was performed by fluorescence microscopy. The cell migration was assessed by quantification of fluorescence microscopy pictures (at least three fields for each determination).

Lipid measurement by liquid chromatography-tandem mass spectrometry (LC-MS/MS)

Analysis of sphingolipids in lipid extracts was performed by LC-MS/MS as described in Ogiso *et al.*[66]

Lipid extraction and determination of phosphatidylinositol 3-phosphate

The culture media were removed, and cells were washed rapidly three times with ice-cold PBS. After protein determination, lipids were extracted *via* the modified method of Bligh and Dyer.[67] Lipids were dried down and resuspended in assay buffer, and then phosphatidylinositol 3-phosphate levels were determined by ELISA kit.

Preparation of expression constructs

PI3KC2β (full length) was amplified by PCR using the sets of primers, EcoRI-start1F (ggtaccgaattcatgtcttcgactcagggcaat) containing an *Eco*RI site, and XhoI-nostop5058R (tctagactcgagcaaggtgccatgacttcg) containing a *Xho*I site without a stop codon. The C2 domain of the N terminus (C2A) was amplified using EcoRI-start1F and reverse primer XhoI-nostop2382R (tctagactcgaggaacttgatgtcaaaggccg). PIK-catalytic domain was amplified using EcoRI-start2437F (ggtaccgaattcatggaagaagaccagcgcaagctta) and XhoI-4431R (tctagactcgagcagtgggtggaagaaggtgta). The region of PIK-catalytic domain upstream from C2B domain (C2B deletion) was amplified using forward primer EcoRI-start1F and the reverse primer XhoI-C2del-4515R (tctagactcgagtcccacctttccgacg) containing a *Xho*I site without a stop codon. Each PCR product and pcDNA3.1/V5-His A were digested with *Eco*RI/*Xho*I and each fragment was ligated. The sequence of the produced plasmid was verified with T7 primer and BGH primer as universal primer.

Transfection with siRNAs or PI3KC2β vectors

For siRNA transfection, SKOV3 cells (2×10^4) grown on glass-bottom dishes were transfected with siRNAs using RNAiMax transfection reagent. For transfection with plasmid vectors, cells (5×10^4) grown on glass-bottom dishes were transfected with 2 μg plasmid vectors using Lipofectamine 2000.

Immunofluorescence

Cells growing on 35-mm glass-bottom dishes were fixed for 10 min at room temperature with 4% formaldehyde in PBS and then washed with PBS. Cells were treated for 10 min with 0.1% TritonX-100, washed with PBS, and blocked for 1 h with PBS containing 2% human serum. Cells were incubated with V5 or phospho-Akt antibodies in PBS containing 2% human serum overnight. After washing with PBS, cells were incubated with Alexa488- and/or Alexa555-conjugated anti-IgG antibodies and Hoechst 33342 in PBS containing 2% human serum for 1 h. Confocal laser microscopy was performed using an LSM780 confocal microscope (Carl Zeiss, Thornwood, NY, USA).

Determination of ceramide-interacting proteins

SKOV3 cells were lysed in RIPA buffer (100 mM NaCl, 1% Triton-X 100, 1% sodium deoxycholate, 0.1% SDS, 1 mM EDTA, 10 mM Tris HCl, pH 7.5) at room temperature. The lysates were centrifuged at 20,000 × *g* for 10 min, and the supernatants (1 mg/ml protein) were treated with 10 μM biotin or C_6-ceramide-conjugated biotin in the presence of streptavidin-conjugated magnetic beads at room temperature for 1 h. The magnetic bead complexes were washed three times with RIPA buffer, and C_6-ceramide-interacting proteins were extracted. The proteins were subjected to immunoblotting using antibodies against PI3KC2β, V5, β-actin, PKCα, and PI3KCα/p110α.

Preparation of ceramide liposomes

Ceramide liposomes conjugated with transferrin and octadecyl-rhodamine B were prepared as described by Koshkaryev *et al.*[27]

Ethics statement

All animal studies were approved by the Institutional Animal Care and Use Committee of Tohoku University, Japan. The ID numbers are 2013MeDo-006 and 2015MeDo-001.

Human ovarian cancer cell xenograft studies

Five-week-old female nude mice (BALB/c; Charles River Japan) were injected intraperitoneally with SKOV3 cells for examination of their peritoneal metastatic potential. For assessing effects of liposomal ceramides on metastasis (Figure 6), five million of the suspended cells were treated with PBS, TLs, or C_6-Cer TLs for 30 min and intraperitoneally inoculated into mice. Mice were randomly allocated to three groups ($n = 12$). For assessing effects of PI3KC2β knockdown on anti-metastatic activities of ceramide liposomes (Figure 7), twenty mice were randomly allocated to four groups ($n = 5$) and siRNA-treated cells (5×10^6 cells) were inoculated into mouse peritoneal. The mice were sacrificed at 4 weeks after inoculation, and the number and extent of overt metastases (>1 mm) were quantified. When inoculation of cells to mouse peritoneal failed, the mice were euthanized and excluded from analysis. Moreover, mice with early death were also excluded from analysis.

Statistical analysis

Data presented in bar graphs represent the mean ± SEM of at least two independent experiments. Pictures presented were representative of at least three independent

experiments. Sample sizes for relevant experiments were determined by power analyses conducted during experiment planning (β = 0.8, $P = 0.05$). Statistical analyses were performed using GraphPad Prism and Instat. Individual t tests were performed for significance assessment of the differences between treatments. All P-values less than 0.05 were considered as significant.

Supplementary Material

Refer to Web version on PubMed Central for supplementary material.

Acknowledgments

This study was supported in part by JSPS KAKENHI Grants (40539235 to K.K., 24390375 to N.Y. and 23791801 to M.T.), a Health Labour Sciences Research Grant (201221019A to N.Y.), and National Institutes of Health grants (U54 CA151881 to V.P.T. and CA087584 to Y.A.H.). We also thank the laboratory members of the Departments of Microbiology and Immunology, and Obstetrics and Gynecology (Tohoku University, Sendai) for critical discussion.

References

1. Lengyel E. Ovarian cancer development and metastasis. Am J Pathol. 2010; 177:1053–64. [PubMed: 20651229]
2. Banerjee S, Kaye SB. New strategies in the treatment of ovarian cancer: current clinical perspectives and future potential. Clin Cancer Res. 2013; 19:961–8. [PubMed: 23307860]
3. Naora H, Montell DJ. Ovarian cancer metastasis: integrating insights from disparate model organisms. Nat Rev Cancer. 2005; 5:355–66. [PubMed: 15864277]
4. Tan DS, Agarwal R, Kaye SB. Mechanisms of transcoelomic metastasis in ovarian cancer. Lancet Oncol. 2006; 7:925–34. [PubMed: 17081918]
5. Yamazaki D, Kurisu S, Takenawa T. Regulation of cancer cell motility through actin reorganization. Cancer Sci. 2005; 96:379–86. [PubMed: 16053508]
6. Wells A, Grahovac J, Wheeler S, Ma B, Lauffenburger D. Targeting tumor cell motility as a strategy against invasion and metastasis. Trends Pharmacol Sci. 2013; 34:283–9. [PubMed: 23571046]
7. Lauffenburger DA, Horwitz AF. Cell migration: a physically integrated molecular process. Cell. 1996; 84:359–69. [PubMed: 8608589]
8. Nurnberg A, Kitzing T, Grosse R. Nucleating actin for invasion. Nat Rev Cancer. 2011; 11:177–87. [PubMed: 21326322]
9. Meyer AS, Hughes-Alford SK, Kay JE, Castillo A, Wells A, Gertler FB, Lauffenburger DA. 2D protrusion but not motility predicts growth factor-induced cancer cell migration in 3D collagen. J Cell Biol. 2012; 197:721–9. [PubMed: 22665521]
10. Hannun YA. Functions of ceramide in coordinating cellular responses to stress. Science. 1996; 274:1855–9. [PubMed: 8943189]
11. Kitatani K, Idkowiak-Baldys J, Hannun YA. The sphingolipid salvage pathway in ceramide metabolism and signaling. Cell Signal. 2008; 20:1010–8. [PubMed: 18191382]
12. Kitatani K, Sheldon K, Anelli V, Jenkins RW, Sun Y, Grabowski GA, Obeid LM, Hannun YA. Acid beta-glucosidase 1 counteracts p38delta-dependent induction of interleukin-6: possible role for ceramide as an anti-inflammatory lipid. J Biol Chem. 2009; 284:12979–88. [PubMed: 19279008]
13. Clarke CJ, Truong TG, Hannun YA. Role for neutral sphingomyelinase-2 in tumor necrosis factor alpha-stimulated expression of vascular cell adhesion molecule-1 (VCAM) and intercellular adhesion molecule-1 (ICAM) in lung epithelial cells: p38 MAPK is an upstream regulator of nSMase2. J Biol Chem. 2007; 282:1384–96. [PubMed: 17085432]
14. Garzotto M, White-Jones M, Jiang Y, Ehleiter D, Liao WC, Haimovitz-Friedman A, Fuks Z, Kolesnick R. 12-O-tetradecanoylphorbol-13-acetate-induced apoptosis in LNCaP cells is mediated through ceramide synthase. Cancer Res. 1998; 58:2260–4. [PubMed: 9605775]

15. Hannun YA, Obeid LM. Principles of bioactive lipid signalling: lessons from sphingolipids. Nat Rev Mol Cell Biol. 2008; 9:139–50. [PubMed: 18216770]

16. Park JW, Park WJ, Futerman AH. Ceramide synthases as potential targets for therapeutic intervention in human diseases. Biochim Biophys Acta. 2014; 1841:671–81. [PubMed: 24021978]

18. Ogretmen B, Pettus BJ, Rossi MJ, Wood R, Usta J, Szulc Z, Bielawska A, Obeid LM, Hannun YA. Biochemical mechanisms of the generation of endogenous long chain ceramide in response to exogenous short chain ceramide in the A549 human lung adenocarcinoma cell line. Role for endogenous ceramide in mediating the action of exogenous ceramide. J Biol Chem. 2002; 277:12960–9. [PubMed: 11815611]

19. Takeda S, Mitsutake S, Tsuji K, Igarashi Y. Apoptosis occurs via the ceramide recycling pathway in human HaCaT keratinocytes. J Biochem. 2006; 139:255–62. [PubMed: 16452313]

20. Kitatani K, Idkowiak-Baldys J, Bielawski J, Taha TA, Jenkins RW, Senkal CE, Ogretmen B, Obeid LM, Hannun YA. Protein kinase C-induced activation of a ceramide/protein phosphatase 1 pathway leading to dephosphorylation of p38 MAPK. J Biol Chem. 2006; 281:36793–802. [PubMed: 17030510]

21. Kitatani K, Idkowiak-Baldys J, Hannun YA. Mechanism of inhibition of sequestration of protein kinase C alpha/betaII by ceramide. Roles of ceramide-activated protein phosphatases and phosphorylation/dephosphorylation of protein kinase C alpha/betaII on threonine 638/641. J Biol Chem. 2007; 282:20647–56. [PubMed: 17504762]

22. Morad SA, Cabot MC. Ceramide-orchestrated signalling in cancer cells. Nat Rev Cancer. 2013; 13:51–65. [PubMed: 23235911]

23. Stover TC, Sharma A, Robertson GP, Kester M. Systemic delivery of liposomal short-chain ceramide limits solid tumor growth in murine models of breast adenocarcinoma. Clin Cancer Res. 2005; 11:3465–74. [PubMed: 15867249]

24. Stover T, Kester M. Liposomal delivery enhances short-chain ceramide-induced apoptosis of breast cancer cells. J Pharmacol Exp Ther. 2003; 307:468–75. [PubMed: 12975495]

25. van Vlerken LE, Duan Z, Seiden MV, Amiji MM. Modulation of intracellular ceramide using polymeric nanoparticles to overcome multidrug resistance in cancer. Cancer Res. 2007; 67:4843–50. [PubMed: 17510414]

26. Boddapati SV, D'Souza GG, Erdogan S, Torchilin VP, Weissig V. Organelle-targeted nanocarriers: specific delivery of liposomal ceramide to mitochondria enhances its cytotoxicity in vitro and in vivo. Nano Lett. 2008; 8:2559–63. [PubMed: 18611058]

27. Koshkaryev A, Piroyan A, Torchilin VP. Increased apoptosis in cancer cells in vitro and in vivo by ceramides in transferrin-modified liposomes. Cancer Biol Ther. 2012; 13:50–60. [PubMed: 22336588]

28. Tran MA, Smith CD, Kester M, Robertson GP. Combining nanoliposomal ceramide with sorafenib synergistically inhibits melanoma and breast cancer cell survival to decrease tumor development. Clin Cancer Res. 2008; 14:3571–81. [PubMed: 18519791]

29. Xue G, Hemmings BA. PKB/Akt-dependent regulation of cell motility. J Natl Cancer Inst. 2013; 105:393–404. [PubMed: 23355761]

30. Rodon J, Dienstmann R, Serra V, Tabernero J. Development of PI3K inhibitors: lessons learned from early clinical trials. Nat Rev Clin Oncol. 2013; 10:143–53. [PubMed: 23400000]

31. Bast RC Jr. Hennessy B, Mills GB. The biology of ovarian cancer: new opportunities for translation. Nat Rev Cancer. 2009; 9:415–28. [PubMed: 19461667]

32. Shayesteh L, Lu Y, Kuo WL, Baldocchi R, Godfrey T, Collins C, Pinkel D, Powell B, Mills GB, Gray JW. PIK3CA is implicated as an oncogene in ovarian cancer. Nat Genet. 1999; 21:99–102. [PubMed: 9916799]

33. Stratford S, Hoehn KL, Liu F, Summers SA. Regulation of insulin action by ceramide: dual mechanisms linking ceramide accumulation to the inhibition of Akt/protein kinase B. J Biol Chem. 2004; 279:36608–15. [PubMed: 15220355]

34. Olson MF, Sahai E. The actin cytoskeleton in cancer cell motility. Clinical & experimental metastasis. 2009; 26:273–87. [PubMed: 18498004]

35. Ip CK, Cheung AN, Ngan HY, Wong AS. p70 S6 kinase in the control of actin cytoskeleton dynamics and directed migration of ovarian cancer cells. Oncogene. 2011; 30:2420–32. [PubMed: 21258406]
36. Yoshizaki H, Mochizuki N, Gotoh Y, Matsuda M. Akt-PDK1 complex mediates epidermal growth factor-induced membrane protrusion through Ral activation. Mol Biol Cell. 2007; 18:119–28. [PubMed: 17079732]
37. Fruman DA, Meyers RE, Cantley LC. Phosphoinositide kinases. Annu Rev Biochem. 1998; 67:481–507. [PubMed: 9759495]
38. Nitta M, Katabuchi H, Ohtake H, Tashiro H, Yamaizumi M, Okamura H. Characterization and tumorigenicity of human ovarian surface epithelial cells immortalized by SV40 large T antigen. Gynecol Oncol. 2001; 81:10–7. [PubMed: 11277643]
39. Wang E, Norred WP, Bacon CW, Riley RT, Merrill AH Jr. Inhibition of sphingolipid biosynthesis by fumonisins. Implications for diseases associated with Fusarium moniliforme. J Biol Chem. 1991; 266:14486–90. [PubMed: 1860857]
40. Wijesinghe DS, Massiello A, Subramanian P, Szulc Z, Bielawska A, Chalfant CE. Substrate specificity of human ceramide kinase. J Lipid Res. 2005; 46:2706–16. [PubMed: 16170208]
41. Niikura H, Sasano H, Sato S, Yajima A. Expression of epidermal growth factor-related proteins and epidermal growth factor receptor in common epithelial ovarian tumors. Int J Gynecol Pathol. 1997; 16:60–8. [PubMed: 8986534]
42. Bartlett JM, Langdon SP, Simpson BJ, Stewart M, Katsaros D, Sismondi P, Love S, Scott WN, Williams AR, Lessells AM, et al. The prognostic value of epidermal growth factor receptor mRNA expression in primary ovarian cancer. Br J Cancer. 1996; 73:301–6. [PubMed: 8562334]
43. Zhou HY, Pon YL, Wong AS. Synergistic effects of epidermal growth factor and hepatocyte growth factor on human ovarian cancer cell invasion and migration: role of extracellular signal-regulated kinase 1/2 and p38 mitogen-activated protein kinase. Endocrinology. 2007; 148:5195–208. [PubMed: 17673518]
44. Enomoto A, Murakami H, Asai N, Morone N, Watanabe T, Kawai K, Murakumo Y, Usukura J, Kaibuchi K, Takahashi M. Akt/PKB regulates actin organization and cell motility via Girdin/APE. Dev Cell. 2005; 9:389–402. [PubMed: 16139227]
45. Zhou H, Summers SA, Birnbaum MJ, Pittman RN. Inhibition of Akt kinase by cell-permeable ceramide and its implications for ceramide-induced apoptosis. J Biol Chem. 1998; 273:16568–75. [PubMed: 9632728]
46. Dobrowsky RT, Hannun YA. Ceramide stimulates a cytosolic protein phosphatase. J Biol Chem. 1992; 267:5048–51. [PubMed: 1312082]
47. Ogretmen B, Hannun YA. Biologically active sphingolipids in cancer pathogenesis and treatment. Nat Rev Cancer. 2004; 4:604–16. [PubMed: 15286740]
48. Bialojan C, Takai A. Inhibitory effect of a marine-sponge toxin, okadaic acid, on protein phosphatases. Specificity and kinetics. Biochem J. 1988; 256:283–90. [PubMed: 2851982]
49. Ishihara H, Martin BL, Brautigan DL, Karaki H, Ozaki H, Kato Y, Fusetani N, Watabe S, Hashimoto K, Uemura D, et al. Calyculin A and okadaic acid: inhibitors of protein phosphatase activity. Biochemical and biophysical research communications. 1989; 159:871–7. [PubMed: 2539153]
50. Salmena L, Carracedo A, Pandolfi PP. Tenets of PTEN tumor suppression. Cell. 2008; 133:403–14. [PubMed: 18455982]
51. Aschrafi A, Franzen R, Shabahang S, Fabbro D, Pfeilschifter J, Huwiler A. Ceramide induces translocation of protein kinase C-alpha to the Golgi compartment of human embryonic kidney cells by interacting with the C2 domain. Biochim Biophys Acta. 2003; 1634:30–9. [PubMed: 14563411]
52. Huwiler A, Fabbro D, Pfeilschifter J. Selective ceramide binding to protein kinase C-alpha and -delta isoenzymes in renal mesangial cells. Biochemistry. 1998; 37:14556–62. [PubMed: 9772184]
53. Huwiler A, Johansen B, Skarstad A, Pfeilschifter J. Ceramide binds to the CaLB domain of cytosolic phospholipase A2 and facilitates its membrane docking and arachidonic acid release. Faseb J. 2001; 15:7–9. [PubMed: 11099485]

54. Arcaro A, Volinia S, Zvelebil MJ, Stein R, Watton SJ, Layton MJ, Gout I, Ahmadi K, Downward J, Waterfield MD. Human phosphoinositide 3-kinase C2beta, the role of calcium and the C2 domain in enzyme activity. J Biol Chem. 1998; 273:33082–90. [PubMed: 9830063]
55. Bader AG, Kang S, Zhao L, Vogt PK. Oncogenic PI3K deregulates transcription and translation. Nat Rev Cancer. 2005; 5:921–9. [PubMed: 16341083]
56. Torchilin VP. Recent advances with liposomes as pharmaceutical carriers. Nat Rev Drug Discov. 2005; 4:145–60. [PubMed: 15688077]
57. Sun Y, Fox T, Adhikary G, Kester M, Pearlman E. Inhibition of corneal inflammation by liposomal delivery of short-chain, C-6 ceramide. J Leukoc Biol. 2008; 83:1512–21. [PubMed: 18372342]
58. Yilmaz M, Christofori G. EMT, the cytoskeleton, and cancer cell invasion. Cancer metastasis reviews. 2009; 28:15–33. [PubMed: 19169796]
59. Maffucci T, Cooke FT, Foster FM, Traer CJ, Fry MJ, Falasca M. Class II phosphoinositide 3-kinase defines a novel signaling pathway in cell migration. J Cell Biol. 2005; 169:789–99. [PubMed: 15928202]
60. Pua TL, Wang FQ, Fishman DA. Roles of LPA in ovarian cancer development and progression. Future oncology. 2009; 5:1659–73. [PubMed: 20001802]
61. Boller D, Doepfner KT, De Laurentiis A, Guerreiro AS, Marinov M, Shalaby T, Depledge P, Robson A, Saghir N, Hayakawa M, et al. Targeting PI3KC2beta impairs proliferation and survival in acute leukemia, brain tumours and neuroendocrine tumours. Anticancer Res. 2012; 32:3015–27. [PubMed: 22843869]
62. Edmond V, Dufour F, Poiroux G, Shoji K, Malleter M, Fouque A, Tauzin S, Rimokh R, Sergent O, Penna A, et al. Downregulation of ceramide synthase-6 during epithelial-to-mesenchymal transition reduces plasma membrane fluidity and cancer cell motility. Oncogene. 2014
63. Maceyka M, Spiegel S. Sphingolipid metabolites in inflammatory disease. Nature. 2014; 510:58–67. [PubMed: 24899305]
64. Calzolari A, Oliviero I, Deaglio S, Mariani G, Biffoni M, Sposi NM, Malavasi F, Peschle C, Testa U. Transferrin receptor 2 is frequently expressed in human cancer cell lines. Blood Cells Mol Dis. 2007; 39:82–91. [PubMed: 17428703]
65. Karahatay S, Thomas K, Koybasi S, Senkal CE, Elojeimy S, Liu X, Bielawski J, Day TA, Gillespie MB, Sinha D, et al. Clinical relevance of ceramide metabolism in the pathogenesis of human head and neck squamous cell carcinoma (HNSCC): attenuation of C(18)-ceramide in HNSCC tumors correlates with lymphovascular invasion and nodal metastasis. Cancer letters. 2007; 256:101–11. [PubMed: 17619081]
66. Ogiso H, Taniguchi M, Araya S, Aoki S, Wardhani LO, Yamashita Y, Ueda Y, Okazaki T. Comparative Analysis of Biological Sphingolipids with Glycerophospholipids and Diacylglycerol by LC-MS/MS. Metabolites. 2014; 4:98–114. [PubMed: 24958389]
67. Bligh EG, Dyer WJ. A rapid method of total lipid extraction and purification. Canadian journal of biochemistry and physiology. 1959; 37:911–7. [PubMed: 13671378]

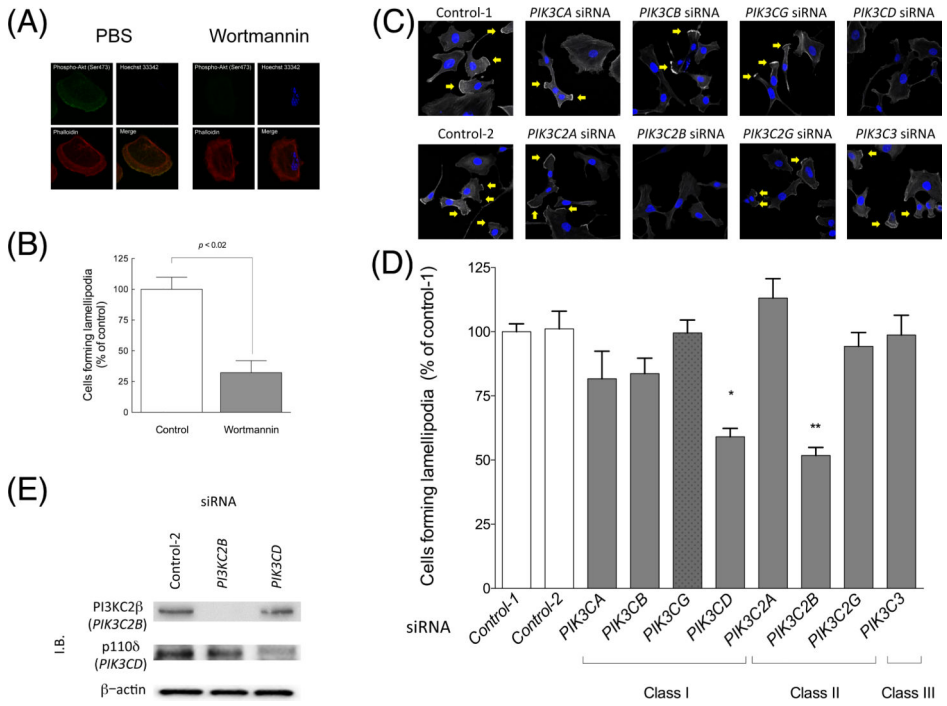

Figure 1. Effects of C_6-ceramide on motility of ovarian cancer cells

(A and B) SKOV3 cells, growing in DMEM supplemented with 10% FBS, were incubated with vehicle (control) or 100 nM wortmannin for 30 min. After treatment, cells were fixed followed by staining with phospho-Akt (green), TRITC-conjugated phalloidin (red) and Hoechst 33342 (blue). Imaging was performed by confocal microscopy, and representative images are shown (A). Formation of lamellipodia was assessed as described in "Materials and Methods" (B). The data shown (mean ± SEM, $n = 3$) are the percentage of cells forming lamellipodia. (C and D) SKOV3 cells were transfected with 20 nM siRNAs for control-1 ($n = 12$), control-2 ($n = 8$), *PIK3CA* ($n = 6$), *PIK3CB* ($n = 4$), *PIK3CG* ($n = 4$), *PIK3CD* ($n = 5$), *PIK3C2A* ($n = 4$), *PIK3C2B* ($n = 7$), *PIK3C2G* ($n = 4$), or *PIK3C3* ($n = 4$). After 48 h transfection, cells were fixed followed by staining with TRITC-conjugated phalloidin (white) and Hoechst 33342 (blue). Imaging was performed by confocal microscopy, and representative images are shown (C). Formation of lamellipodia was assessed as described in "Materials and Methods" and yellow allows show lamellipodia (D). Data shown (mean ± SEM, at least four independent experiments) are the percentages relative to cells treated with control-1 siRNAs. Statistical analyses were performed by unpaired, student *t*-test. *, $P < 0.02$ and $P < 0.001$ compared with control-1 and control-2, respectively; **, $P < 0.02$ and $P < 0.002$ compared with control-1 and control-2. (E) SKOV3 cells were transfected with the indicated siRNA for 48 h. Extracted proteins were submitted to immunoblot analysis using antibodies specific for PI3KC2β (*PIK3C2B*) and p110δ (*PIK3CD*), and β-actin. Equal amounts of protein were loaded in each lane. Results are representative of three independent experiments.

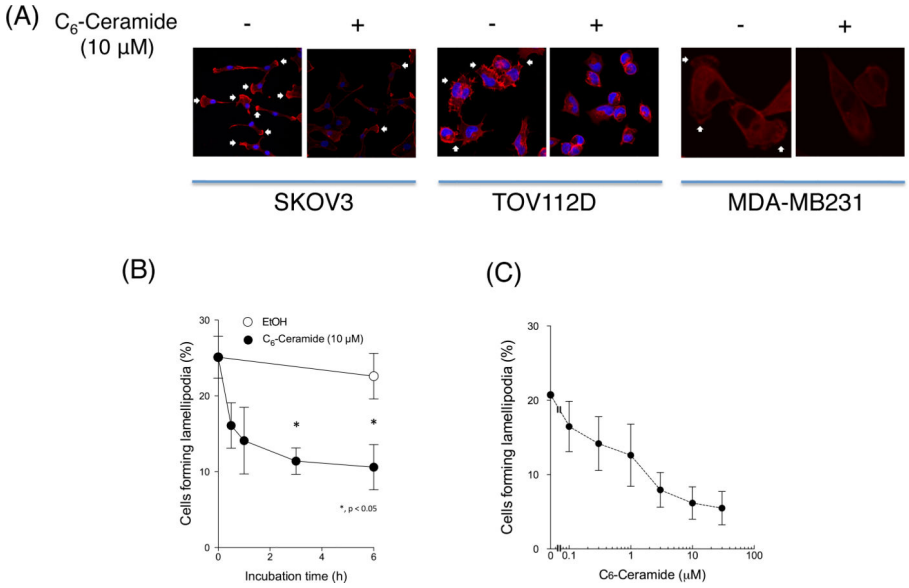

Figure 2. Effects of C_6-ceramide on formation of pseudopodia, including lamellipodia and filopodia, in ovarian and breast cancer cells

(A) SKOV3, TOV112D, and MDA-MB-231 cells were treated with or without 10 μM C_6-ceramide for 3 h. Cells were fixed followed by staining with TRITC-conjugated phalloidin (red) and Hoechst 33342 (blue). Imaging was performed by confocal microscopy and results are representative of three independent experiments. White allows show lamellipodia. (B and C) SKOV3 cells, grown in DMEM supplemented with 10% FBS, were treated with 10 μM C_6-ceramide for the indicated times (B) or with the indicated concentrations of C_6-ceramide for 3 h (C). Formation of lamellipodia was assessed as described in "Materials and Methods". The data shown (mean ± SEM) are the percentages of cells forming lamellipodia. Four or three independent experiments were performed. Statistical analyses were performed by unpaired, student *t*-test. *, $P < 0.05$. A, $n = 7$ for vehicle, $n = 8$ (0.5 h), 8 (1 h), 13 (3 h), 13 (6 h) for C_6-ceramide; B, $n = 3$.

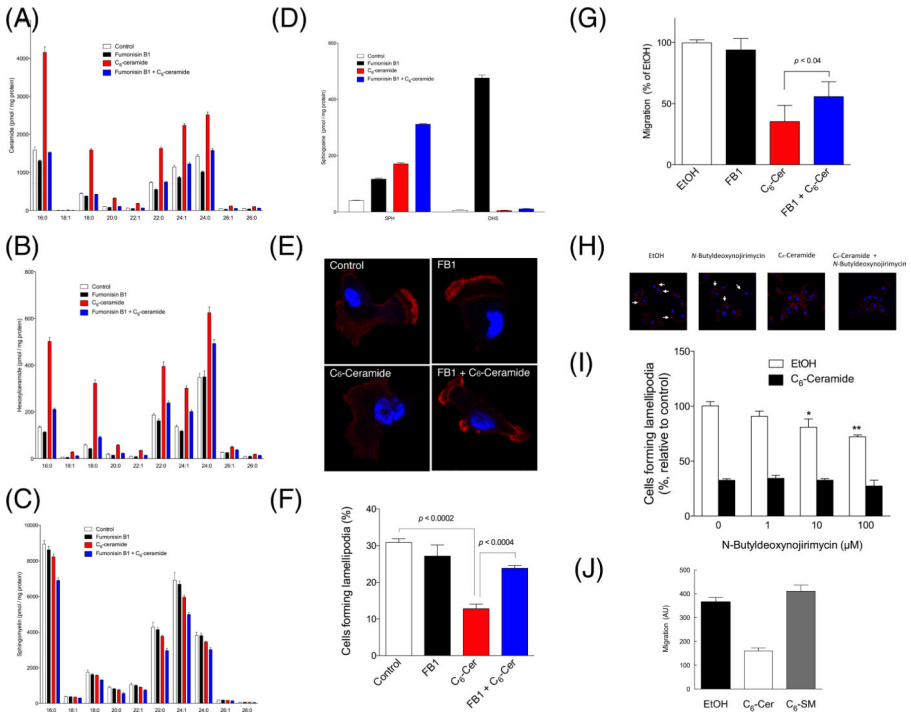

Figure 3. Identification of ceramide as an inhibitory lipid in cell motility of ovarian cancer cells

SKOV3 cells were simultaneously treated with or without 200 μM fumonisin B1 (FB1) in the absence or presence of 10 μM C_6-ceramide for 3 h. (A–D) Lipids were extracted from cells and then sphingolipids (A, long-chain ceramide; B, long-chain hexosylceramide; C, long-chain sphingomyelin; D, sphingosine) were determined by MS. Values are means ± SEM (two independent experiments, $n = 4$). (E and F) Cells were fixed and stained with TRITC-conjugated phalloidin (red) and Hoechst 33342 (blue). Representative images are shown (E). Formation of lamellipodia was assessed as described in "Materials and Methods" (F). Data shown (mean ± SEM, at least three independent experiments are the percentages of cells forming lamellipodia. $n = 3$ (Control), 5 (FB1), 4 (C_6-Cer), 4 (FB1+C_6-Cer). (G) Cell migration was assessed as described in "Materials and Methods". Data shown (mean ± SEM, four independent experiments, $n = 4$) are the percentages of vehicle control cells (0.1% ethanol treatment). (H and I) SKOV3 cells were simultaneously treated with 10 μM C_6-ceramide in the absence or presence of N-butyldeoxynojirimycin for 3 h. Cells were fixed and stained with TRITC-conjugated phalloidin (red) and Hoechst 33342 (blue). Representative images are shown and white allows show lamellipodia. Formation of lamellipodia was assessed as described in "Materials and Methods". Data shown (mean ± SEM, three independent experiments, $n = 3$) are the percentages relative to EtOH. *, $P <$ 0.0001, **, $P < 0.002$ compared with EtOH. (J) SKOV3 cells were incubated with vehicle (0.1% ethanol), 10 μM C_6-ceramide (C_6-Cer) or C_6-sphingomyelin (C_6-SM) for 3 h. Cell migration was assessed as described in "Materials and Methods". Data shown (mean ± SEM, three independent experiments, $n = 3$) are percentages of vehicle control cells (0.1% ethanol treatment). Statistical analyses were performed by unpaired, student *t*-test.

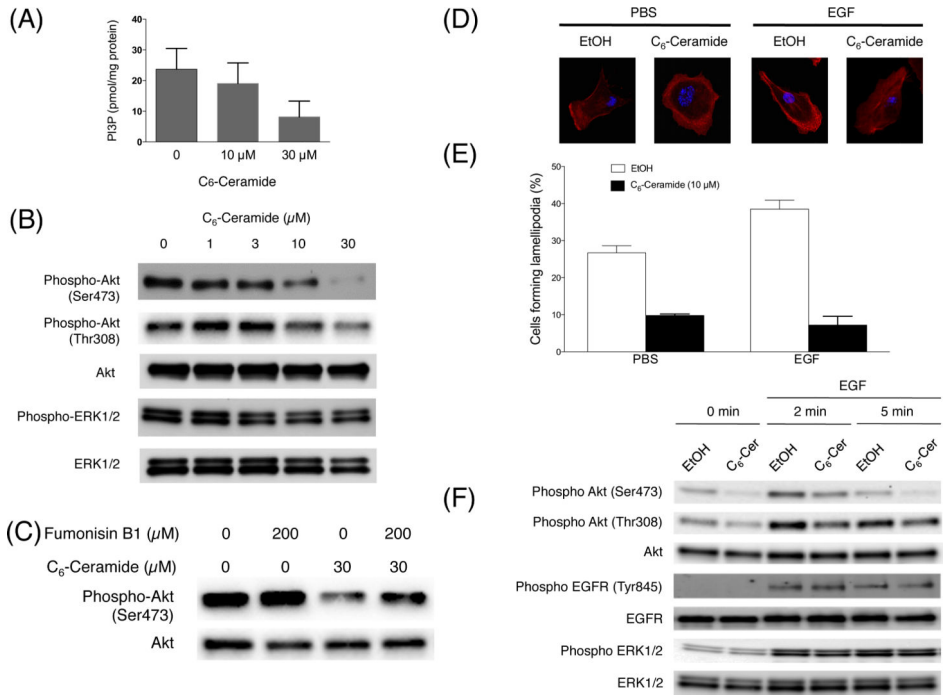

Figure 4. Effects of ceramide on PI3K signaling in ovarian cancer cells

(A) SKOV3 cells were incubated with 10 μM C_6-ceramide for 3 h. After treatment, lipids were extracted and phosphatidylinositol 3-phosphate mass was determined by ELISA. Results represent mean ± SEM (two independent experiments, $n = 4$). (B) SKOV3 cells were treated with the indicated concentration of C_6-ceramide for 3 h. Extracted cellular proteins were submitted to immunoblot analysis using antibodies specific for phospho-Akt at Ser^{473} or Thr^{308}, Akt, phosphor-ERK1/2, and ERK1/2. Equal amounts of protein were loaded in each lane. Results are representative of three independent experiments. (C) SKOV3 cells were simultaneously treated with or without 200 μM fumonisin B1 (FB1) in the absence or presence of 10 μM C_6-ceramide for 3 h. Whole-cell lysates were prepared and subjected to immunoblot analysis with antibodies specific for phospho-Akt and Akt. Equal amounts of protein were loaded in each lane. Results are representative of four independent experiments. (D and E) SKOV3 cells were incubated with or without 10 μM C_6-ceramide for 3 h followed by treatment with or without 100 ng/ml EGF for 5 min. Cells were fixed and stained with TRITC-conjugated phalloidin (red) and Hoechst 33342 (blue). Representative images are shown (D). Formation of lamellipodia was assessed as described in “Materials and Methods” (E). Data shown (mean ± SEM, three independent experiments, $n = 3$) are the percentages of cells forming lamellipodia. (F) SKOV3 cells were incubated with or without 10 μM C_6-ceramide for 3 h followed by treatment with 100 ng/ml EGF for 2 or 5 min. Proteins were subjected to immunoblot analysis with antibodies specific for phospho-Akt, Akt, and phospo-ERK1/2, ERK1/2, phospho-EGF receptor (EGFR), and EGFR. Equal amounts of protein were loaded in each lane. Results are representative of three independent experiments.

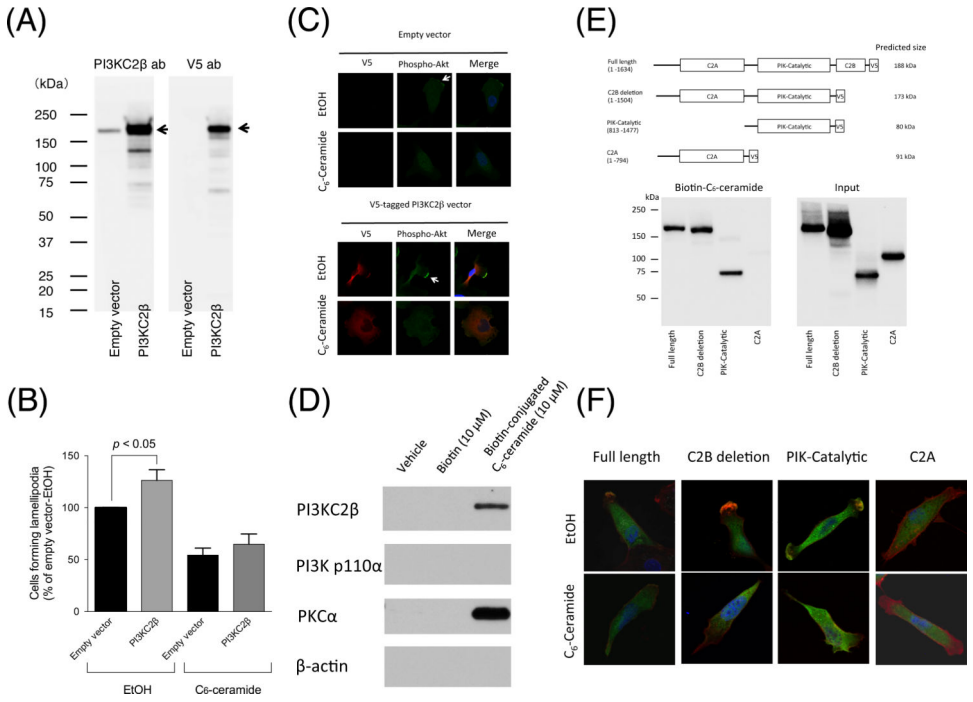

Figure 5. Ceramide interaction with PI3KC2β suppresses cell motility

(A) SKOV3 cells were transfected with empty or V5-tagged PI3KC2β expression vectors. Extracted proteins were submitted to immunoblot analysis with antibodies specific to PI3KC2β or V5. (B) SKOV3 cells transfected with empty or V5-tagged PI3KC2β expression vectors were treated with or without 10 μM C_6-ceramide for 3 h. After cell fixation, cells were stained with TRITC-conjugated phalloidin (red) and Hoechst 33342 (blue). Formation of lamellipodia was assessed as described in “Materials and Methods”. Data shown (mean ± SEM, eight independent experiments, $n = 8$) are the percentages of cells forming lamellipodia. Statistical analyses were performed by unpaired, student t-test. (C) SKOV3 cells transfected with full-length PI3KC2β were treated with vehicle (ethanol) or 30 μM C_6-ceramide for 3 h. After cell fixation, cells were stained with Hoechst 33342 (blue) and antibodies specific for V5 antibody (green) and phospho-Akt (Ser^{473}) (red). Arrows show lamellipodia. Results are representative of two independent experiments. (D) Cell supernatants from SKOV3 cells were treated with DMSO, 10 μM biotin, or 10 μM biotinylated C_6-ceramide for 1 h at room temperature. Ceramide-interacting proteins were pulled down and submitted to immunoblot analysis using antibodies specific for PI3KC2β, PI3KCα (p110α), and PKCα. Results are representative of three independent experiments. (E) Deletion mutant vectors were constructed. Cell supernatants from SKOV3 cells transfected with those vectors were treated with DMSO, 10 μM biotin, or 10 μM biotinylated C_6-ceramide for 1 h at room temperature. Ceramide-interacting proteins were pulled down and submitted to immunoblot analysis using V5 antibody. Results are representative of three independent experiments. (F) SKOV3 cells transfected with the indicated vectors were treated with vehicle (ethanol) or 30 μM C_6-ceramide for 3 h. After fixation, cells were stained with V5 antibody (green), TRITC-conjugated phalloidin (red) and Hoechst 33342 (blue). Results are representative of three independent experiments.

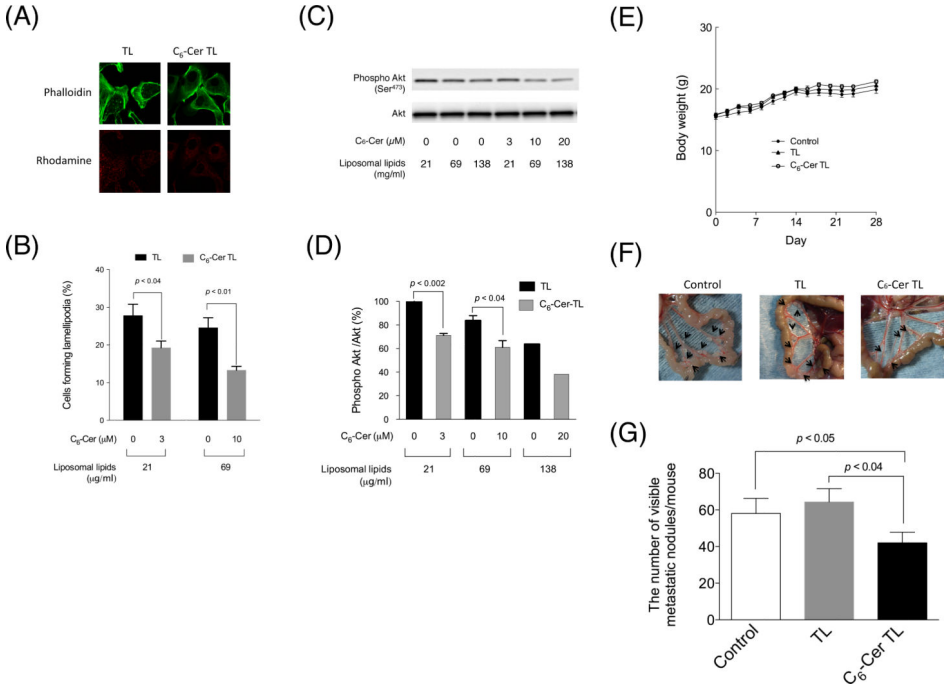

Figure 6. Anti-metastatic effects of ceramide liposomes *in vitro* and *in vivo*

(A–D) SKOV3 cells were incubated with TLs or C_6-Cer TLs for 12 h. Cells were fixed and stained with Alexa-488-conjugated phalloidin (green). Rhodamine (red) shows the uptake of TLs and C_6-Cer-TLs. Imaging was performed by confocal microscopy, and representative images are shown (A). Formation of lamellipodia was assessed as described in "Materials and Methods". Data shown (mean ± SEM, three independent experiments, $n = 3$) are the percentages of cells forming lamellipodia (B). Proteins were subjected to immunoblot analysis with antibodies specific for phospho-Akt at Ser^{473} and Akt. Representative blot images are shown (C). Band signals for phospho-Akt at Ser^{473} and Akt were quantified, and phospho-Akt/Akt values were calculated. Data shown (mean ± SEM, $n = 3$ for 21 and 69 μg/ml lipids liposomal lipids, $n = 1$ for 138 μg/ml lipids liposomal lipids,) are the percentages of phospho-Akt/Akt values relative to TL treatment (21 μg/ml liposomal lipids) (D). (E–G) SKOV3 cells were inoculated into nude mice. Mice were treated with PBS (control, $n = 11$), TLs (15 mg/kg, $n = 8$), C_6-Cer TLs (15 mg/kg, $n = 12$) every other day. Body weight was measured every other day (E). Four weeks later, mice were sacrificed, and the number of metastatic nodules was determined (F and G). Arrows show metastatic nodules. Statistical analyses were performed by unpaired, student *t*-test. *P*-values were shown in Figure.

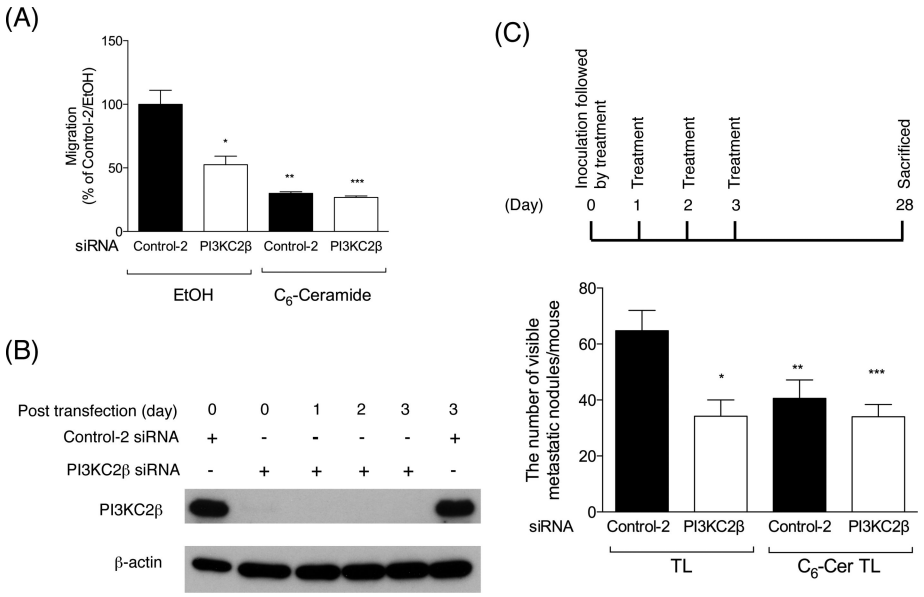

Figure 7. Effects of ceramides on the metastasis of PI3KC2β-silenced cells

(A) SKOV3 cells were transfected with 5 nM control-2 or PI3KC2β siRNAs for 48 h followed by treatment with vehicle (ethanol) or 30 μM C_6-ceramide for 3 h. Cell migration was assessed as described in "Materials and Methods". Data shown (mean ± SEM, four independent experiments, $n = 4$) are the percentages of vehicle control cells (0.1% ethanol treatment). Cell migration in control-2 group was compared with other groups: *$P < 0.02$; **$P < 0.0008$; ***$P < 0.0007$. (B) SKOV3 cells were transfected with 5 nM control-2 or PI3KC2β siRNAs for 24 h and then transfection reagents were removed. Cells were cultured for up to 3 days. Extracted proteins were subjected to immunoblot analysis with PI3KC2β antibody. Results are representative of two independent experiments. (C) SKOV3 cells transfected with siRNAs were inoculated into nude mice. The mice were treated with 15 mg/kg TLs (15 mg/kg, $n = 5$) or C_6-Cer TLs (15 mg/kg, $n = 5$) on the indicated days. Four weeks later after inoculation, mice were sacrificed and the number of metastatic nodules was determined. Metastasis in control-2 group was compared with other groups: *$P < 0.02$; **$P < 0.05$; ***$P < 0.007$. All statistical analyses were performed by unpaired, student *t*-test.